

DEVELOPMENT OF INJURY CRITERIA FOR FRONTAL IMPACT USING A HUMAN BODY FE MODEL

Eric Song

Erwan Lecuyer

Xavier Trosseille

LAB Peugeot Citroën Renault

France

Paper Number 11-0330

ABSTRACT

Sternal deflection is an injury criterion used in current regulatory and consumer tests worldwide to assess thoracic injury risk. However, this criterion has some serious limits when applied to the Hybrid-III dummy: the risk curve based on the criterion is restraint dependent, and it does not allow discrimination between some advanced restraint systems. The THOR dummy, despite its better biofidelity, is confronted with similar limits. This paper presents a study aiming at identification of more robust injury criteria. A human body FE model-based approach was used to achieve this objective. First, an existing human model was updated and validated for frontal impact simulation, not only in terms of its gross motion response, but also in terms of its capability to predict rib fractures. It was then submitted to a wide range of loading types: impactor, static airbag, belt only restraint, airbag only restraint and combined belt and airbag restraint. For each loading type, different loading severities were applied to generate different levels of rib fracture: from the absence of fractures to numerous fractured ribs. Based on these simulations, bending was identified as the main loading pattern for rib fracture, and two injury criteria were formulated: the Combined Deflection (Dc) and the Number of Fractured Ribs (NFR). The Dc is a deflection-based criterion which takes into account not only sternal deflection, but also the effect of asymmetrical loading. This effect can be characterized by L-R differential deflection (difference of thoracic deflections measured on the left side and the right side of the thorax). The NFR is a rib strain-based criterion which intrinsically reflects the injury level of ribs. The simulations showed that the maximum peak strain of all ribs does not correlate with the number of fractured ribs. The NFR can be calculated by measuring dummy rib strain and by fixing a strain threshold beyond which a dummy rib is considered fractured. A possible approach to apply the NFR to mechanical dummies was proposed. However, based entirely on numerical simulations, the findings of this study need to be evaluated by physical testing. A preliminary study on THOR rib strain measurement showed positive signs for implementation of the NFR on the THOR dummy.

INTRODUCTION

Sternal deflection is an injury criterion used in current regulatory and consumer tests (such as US-NCAP, EURO-NCAP ...) worldwide to assess thoracic injury risk. However, this criterion has some serious limits regarding its applications.

Kent et al. (2003) showed that the risk curve in terms of sternal deflection is restraint dependent when measured with the Hybrid-III (H-III) dummy. The risk curve relative to belt loading is completely different from that of airbag loading and that of combined belt and airbag loading. This dependency on the restraint type raises a question as to the relevance of the criterion for its use with the H-III dummy. It means that it is not relevant to construct injury risk curve by mixing data relative to different loading types. It means also that it is incorrect to compare injury risk between these loading types using an injury risk curve constructed in this way.

A more elaborated injury criterion, Cmax (maximum chest compression), was evaluated by Kent et al. (2003) based on 93 cadaver tests. They found that the Cmax is not sensitive to loading types when measured on cadavers. Bose et al. (2009) studied the application of the Cmax on the THOR dummy and found that the risk curve is also restraint-dependent with the dummy.

This study aimed to investigate the relationship between the number of rib fractures and the thoracic deformation in frontal impact, and in particular its variability with respect to various loading types. A finite element thorax model was used to perform this study. It is difficult to use existing biomechanical data for such a study due to: 1) the limited number of PMHS tests available, 2) the important individual variation among PMHS subjects in anthropometry and in mechanical resistance, 3) the lack of the thoracic deflection measurement, or the difficulty to compare them between different methods of measurement when they are available, 4) the uncertainty in the measurements obtained, 5) the different methods used to identify rib fractures. By using a human body model to deal with this issue, one can examine effects of various loading types on a unique subject, with a uniform and accurate

measurement of the thoracic deflection. However, such an approach should be conducted with a thorax model validated not only in terms of global responses but also in terms of injury occurrence, and this for a large range of loading configurations.

Different finite elements thorax models were reported in the literature (Plank and Eppinger 1989, Huang et al. 1994, Lizée et al. 1998, Ruan et al. 2003, Kimpara et al. 2005). These models focused mainly on the validation in terms of global responses, such as the global thorax deflection and the global impact force. Few were dedicated to the validation in terms of injury outcome.

In the current study, an existing human body model (Song et al. 2009) was first updated and validated for frontal impact simulation, not only in terms of its gross motion response, but also in terms of its capability to predict rib fractures. This model was then submitted to a wide range of loading types: impactor, static airbag, belt only restraint, airbag only restraint and combined belt and airbag restraint. For each loading type, different loading severities were applied to generate different levels of rib fracture: from the absence of any fractures to numerous fractured ribs. Based on these simulations, the injury mechanism of rib fractures was investigated, and two candidates are presented respectively as global injury criteria: one based on global thoracic deflection measurement, and the other based on rib strain measurement along the ribs.

EVALUATION OF HUMOS2LAB HUMAN BODY MODEL

The thorax model used in this study was an improved version of the HUMOS model. The HUMOS model is a full human body finite elements model developed by a consortium of universities, research institutes and car manufacturers (Robin 2001). Its mesh was constructed based on the geometry of a single subject who's mass, stature and seated height were close to the mean for a European male. However, the subject presented a more massive torso and less massive lower extremities, typical for an aged person. LAB (Laboratory of Accidentology and Biomechanics) was in charge of the shoulder and the thorax modeling in the first phase of the HUMOS model development in the Radioss™ FE code. The HUMOS model was scaled to other body sizes, and was further updated with respect to new biomechanical data available in the following phases of its development (Vezin et al. 2005). The HUMOS 50th percentile male model in the Radioss™ code was used in this study. Regarding the thorax part of the HUMOS model, the cortical bone of the ribs and the sternum was represented by shell elements, and the trabecular bone by solid

elements. The cartilage between the sternum and the ribs was also represented by solid elements. The muscles and internal organs, such as the heart, lungs, stomach and liver were represented by solid elements. An elasto-plastic material law was used to model the cortical bone, an elastic material law for the trabecular bone and cartilage, and a Boltzman material law for the organs and muscles. The vertebrae were considered as rigid bodies, the connections between them were modeled with general springs. The same was done for the connections between the ribs and the vertebrae. Figure 1 provides an overall view of the HUMOS 50th male model, and Figure 2 shows the thorax part of the model.



Figure 1. Overall view of the Radioss™ HUMOS 50th male model.

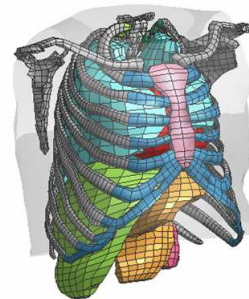


Figure 2. Thorax part of the HUMOS model.

A number of modifications were made to the HUMOS model at the LAB to make the model representative of the behavior of a human thorax, not only in terms of global responses, but also in terms of local responses, such as the strain profiles and rib fractures (Song et al. 2009). To facilitate the expression, the modified model will be referred as the HUMOS2LAB model in the following sections.

In the current study, the HUMOS2LAB model was slightly modified: the cortical bone thickness of first ring of ribs was increased from 0.5 mm to 3 mm; the stiffness of the joint between these ribs and the first dorsal vertebrae was also increased. These modifications were introduced to offer a

more resistant support to the clavicle when the model was subjected to high shoulder belt loading in sled test configuration. They did not change the general validation level of the HUMOS2LAB model. Some examples of validation results of the modified HUMOS2LAB model are provided in Appendix A:

Figure A1 compares the global responses of the HUMOS2LAB model to those of cadaver tests performed by Shaw et al. 2009. Compared responses include: upper and lower shoulder belt forces, sternal deflection, upper left and right thoracic deflection, lower left and right thoracic deflection. A good agreement was observed between model responses and PMHS responses. In particular, the asymmetric deflection pattern of the lower ribcage - characterized by compression on belted side of the ribcage and bulging-out on unbelted side – was well produced.

Figure A2 compares the local strain profile of the 5th rib ring between the thorax model and the cadaver tests under static airbag loading performed by Trosseille et al. 2009. A positive strain corresponds to tension and a negative strain to compression. It can be observed that the model is appropriate to represent the state of deformation for this loading type: the regions of tension and compression, as well as the relative magnitude of strain match the experimental data well.

Figures A3 compares rib fracture regions given by the thorax model to those given by a cadaver test for the frontal sled test with 6kN belt load limiter (Petitjean et al. 2002). In the model, a fracture was established when a shell element of the ribs was deleted. Similar fracture regions were observed.

Figure A4 compares the model responses to those of the experiments (Kroell et al. 1974, Bouquet et al. 1998, Trosseille et al. 2009) in terms of the number of separated fractured ribs (NSFR) versus the impact velocity for the impactor loading type. In the model, a ‘separated’ fracture was established when a pair of face to face shell elements in the external and internal side of rib were deleted. A reasonable agreement between the model responses and the experiments were observed.

In summary, the validation approach used to validate the HUMOS2LAB model represents a significant advance with respect to the classic approach, which is focused mainly on the validation in terms of global responses. It allowed evaluation of the relevance of a thorax model at deeper layers: the interaction between the ribcage and the surrounding tissues, the ribcage deformation, the occurrence and the variation in location of rib fractures versus loading type and

severity. Overall, the thorax model was shown to be consistent with the main features of current cadaver test data available at the LAB, and can be considered as representative of the thoracic behavior.

INJURY MECHANISM OF RIB FRACTURES

It is generally agreed that an excessive strain leads to failure. It is reasonable to extend this general principle to ribs. However, it is not clear how an excessive rib strain is generated in a crash event. In others words, we do not know what type of loading is responsible for excessive strain of ribs. Is it traction, compression, bending, torsion, or a combination of two or more loading modes?

In the HUMOS2LAB model, plastic strain was used as a failure criterion of shell elements representing cortical bones of ribs. A rib fracture occurs when equivalent strain reaches the specified threshold of plastic strain. Consistence of rib fracture regions between the HUMOS2LAB model and PMHS tests observed in the model validation phase supports that excessive strain explains rib fracture well.

Using the HUMOS2LAB model, longitudinal rib strain (along the rib curvilinear axis) and transverse rib strain (along the rib cross section circumference) were compared. Figure 3 is an example of this type of comparison. It shows that the longitudinal strain is the main component compared to the transverse strain. Extensive examination of this type of comparison confirms the generality of this observation. It implies that measurement of strain along the rib axis is a good descriptor of strain state.

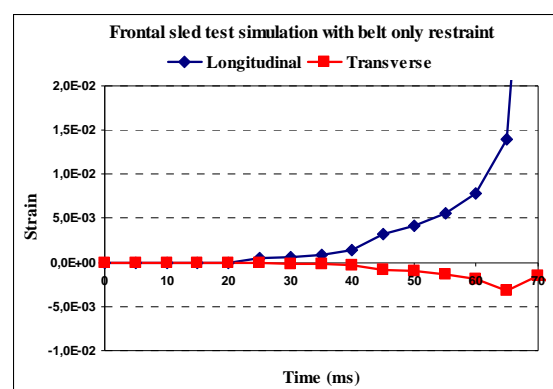
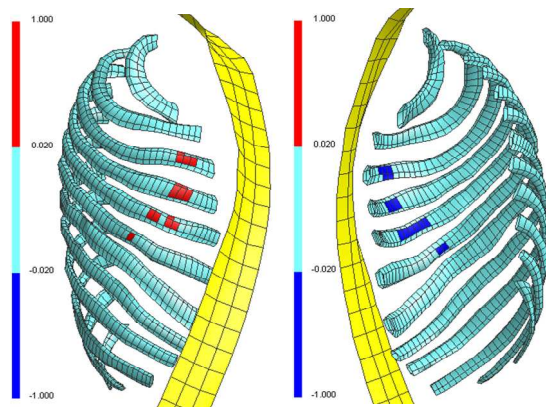


Figure 3. Comparison of the longitudinal rib strain to the transverse rib strain in the same shell element representing rib cortical bone.

In order to determine the loading modes responsible for excessive rib strain, the longitudinal strain field was examined for different HUMOS2LAB model simulations. Bending was identified as an injury mechanism in rib fractures.

Figure 4 is an example for belt loading in a frontal sled test simulation, where high longitudinal strain ($\geq 2\%$) locations are indicated in red (for traction) and in blue (for compression). One can observe that red elements and blue elements are in the opposite sides for each rib. Figure 5 plots stress in face to face shell elements at one of the rib fracture locations. It shows that the traction stress level in the external side of rib is close to the compression stress level in the internal side of rib. These characteristics were also observed for airbag only loading and for combined belt and airbag loading. Based on these observations, it can be concluded that excessive rib strain (or rib fracture) is mainly generated by bending.



Frontal sled with belt

Figure 4. Longitudinal strain field of ribs showing that bending is the main loading mode leading to rib fracture: external side of ribs (left figure), internal side of ribs (right figure).

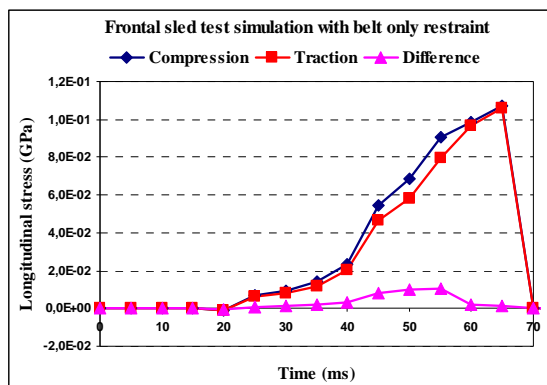


Figure 5. Stress recorded in face to face shell elements at one of the rib fracture locations for belt loading in a frontal sled test simulation.

IDENTIFICATION OF A DEFLECTION-BASED INJURY CRITERION

Simulation matrix

The HUMOS2LAB model was used to identify a global injury criterion correlated to rib fractures but

independent to loading types. That means: the relationship between the number of fractured ribs and the injury criterion candidate should be relatively stable. In other words, it should not depend on loading type. For this purpose, the HUMOS2LAB model was submitted to different loading types:

- Static impactor
- Static airbag
- Belt only restraint in dynamic sled environment
- Airbag only restraint in dynamic sled environment
- Combined belt and airbag restraint dynamic sled environment

These loading types cover the main loading configurations used for PMHS tests in literature, but also current restraint systems used for frontal impact protection. For each loading type, different loading severities were applied in order to generate different levels of ribcage damage: from the absence of any fractures to numerous fractured ribs.

Two series of simulations were carried out. One series corresponds to a plastic strain threshold of 1.3%, another to a plastic strain threshold of 2.4%. The reason of varying the plastic strain threshold is to examine the influence of body resistance level on the injury criterion. The plastic strain threshold of 1.3% is the value used by the HUMOS2LAB model resulting from its validation. It reflects the threshold for fragile subjects since all PMHS tests used to validate the model were carried out with aged subjects. The plastic strain threshold of 2.4% corresponds to an ultimate failure strain of 3.1%, which is in line with experimental data on bones (Burstein et al. 1976) for a middle age subject (around 45 year old). Tables A1 summarizes the simulations performed with plastic strain threshold of 1.3% and corresponding injury outcome. Table A2 gives similar results with the plastic strain threshold of 2.4%. The injury outcome is expressed by the number of fractured ribs. A rib is considered as fractured when a separated fracture occurs on it. A separated fracture was established when a pair of inside and outside face to face shell elements were deleted.

Thoracic deflection measurement

Springs with null stiffness were defined over the ribcage to measure its global deflection at different locations. Each spring records the relative displacement of the node, on which the spring is connected, with respect to the corresponding vertebra, but also with respect to its posterior extremity in order to exclude the rigid body

movement of the rib relative to the vertebra. For example, the springs of the 5th rib measure the relative motion of the nodes relative to the 5th vertebra and the posterior extremity of the 5th rib. The floating ribs were not assessed for this study. The thoracic deflection was measured at 4 different locations for each rib, apart from the first ribs where it was measured only at two locations. To facilitate presentation and discussion, the deflections measured for each rib were noted as D1, D2, D3 and D4, respectively. Figure 6 is an example for the 5th rib ring. For the first ribs, the deflections were noted as D1 and D2 in a similar way.

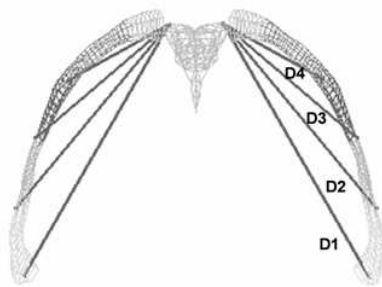


Figure 6. Position of springs measuring the global deformation of the ribcage at the 5th rib level.

More springs were defined over the ribcage to measure its global deflection in its anterior-posterior direction. They are:

- Deflection between the extremity rib 1 and the vertebrae T1
- Deflection between the extremity rib 3 and the vertebrae T4
- Deflection between the extremity rib 5 and the vertebrae T8
- Deflection between the extremity rib 7 and the vertebrae L1
- Deflection between the extremity rib 9 and the vertebrae L2

Three springs were also defined to measure thoracic deflection at levels of the upper sternum, the mid-sternum and the lower sternum.

Based on these measurements, different indicators characterizing thoracic deflection can be defined and calculated.

Injury curve and injury risk curve

In order to examine whether an injury criterion is loading type-dependent, we are going to use a concept named “injury curve”. An injury curve is defined as the relationship between injury outcome and injury predictor. Regarding rib fractures, it is

the number of fractured ribs that is used to express injury outcome. Figure 7 is an example of an injury curve for airbag only restraint in a dynamic sled environment.

The traditional injury risk curve was also used to evaluate loading dependency of an injury predictor. Since a human body model represents a single subject (there is no individual dispersion), the resulting risk curve always presents a vertical slope which separates injury area from non-injury area. The injury risk is either 0% or 100%, and there is no intermediate risk level. Figure 8 is an example of such a risk curve.

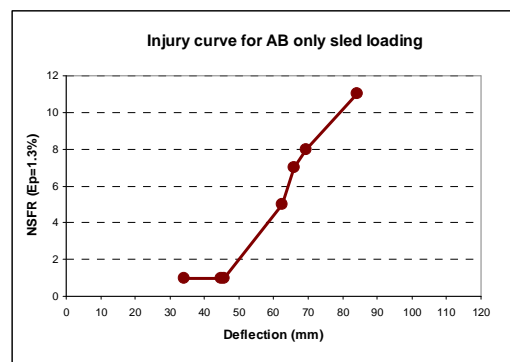


Figure 7. Example of injury curve for airbag only restraint in a dynamic sled environment.

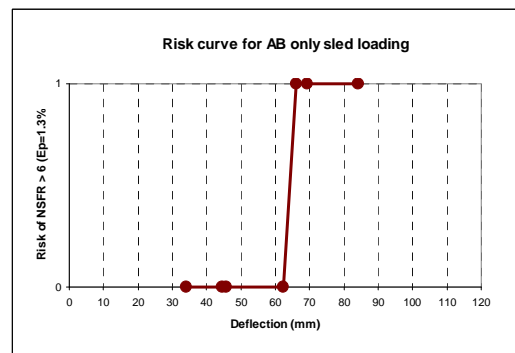


Figure 8. Example of risk curve for airbag only restraint in a dynamic sled environment.

Sternal deflection

Figure 9 shows injury curves and risk curves established based on these simulations in terms of sternal deflection (X-component of the mid-sternum displacement relative to the spine in anterior-posterior direction) for a fragile subject. It can be observed that the injury curve and the risk curve vary from one loading type to another, the 6kN belt loading presenting the most notable difference. The same observation can be made for a stronger subject in Figure 10. Based on these observations, it can be concluded that the sternal

deflection presents, to some extent, signs of loading-type dependent metric. Considering the limits of the criterion when used on H-III and

THOR dummies, a loading-type independent criterion needs to be identified.

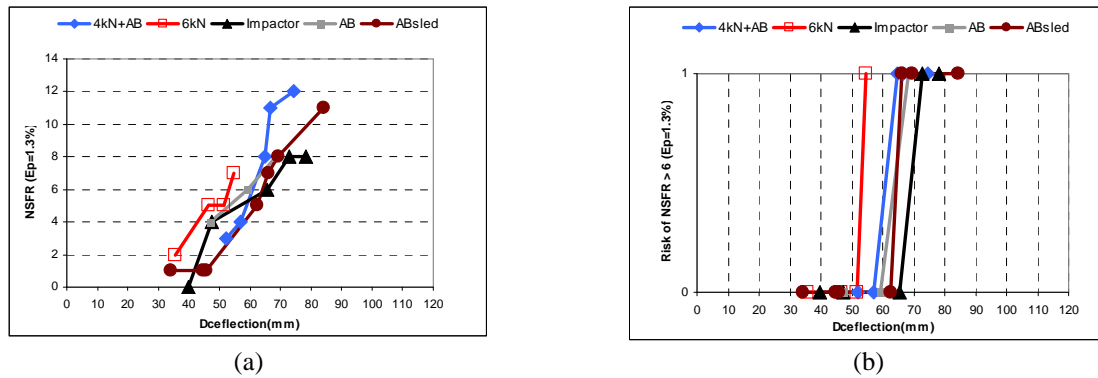


Figure 9. Injury curves (a) and risk curves of NSFR>6 (b) with sternal deflection as injury criterion. The plastic strain failure threshold was fixed at 1.3%, representing a fragile subject.

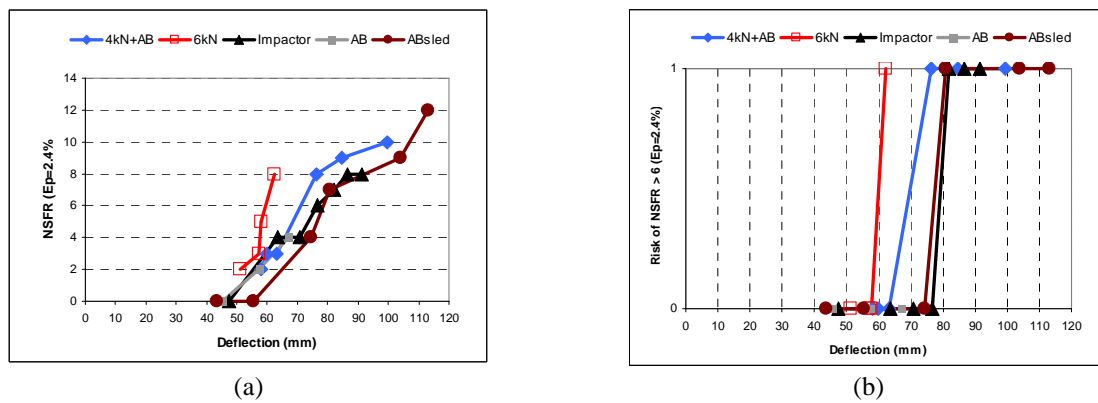


Figure 10. Injury curves (a) and risk curves of NSFR>6 (b) with sternal deflection as injury criterion. The plastic strain failure threshold was fixed at 2.4%, representing a stronger subject.

Combined deflection - a new injury criterion candidate

Simulations with HUMOS2LAB model allow examination of the ribcage deformation shape under different loading types. Figure 11 compares these deformation shapes. It can be observed that important asymmetric deformation was associated with restraints containing a belt, and in particular with a belt only restraint. Tests with cadavers also showed this type of thorax deformation shape under belt loading (Shaw et al. 2009).

Based on these observations, a new injury criterion candidate, named the Combined Deflection and noted as Dc, was defined as below:

$$D_c = D_s + C_f \times [(dD - L_c) + |(dD - L_c)|]$$

Where:

Ds represents the sternal deflection (i.e. the X-component of the mid-sternum displacement relative to the vertebrae T8). This deflection reflects

the amplitude of the symmetric part of the ribcage deflection.

dD, named the differential deflection, is the difference between right and left deflections of lower ribcage measured at the junction between the 7th ribs and the cartilage (i.e. the X-components relative to the vertebrae L1). This deflection reflects the amplitude of the asymmetric part of the ribcage deflection.

The X-axis of the coordinate systems for Ds and dD are oriented to be perpendicular to the sternum at the beginning of a test.

Lc, named the characteristic length, serves to amplify the differentiation effect of the term “dD-LC” between different types of asymmetric loadings.

Cf, named the contribution factor, is a coefficient to weight the contribution of the differential deflection to the Dc.

The Dc was calculated for each simulation performed with HUMOS2LAB model, Lc being fixed at 24 mm, and Cf at 0.15. These values were chosen to give the best result in terms of independency for the various loading types. Figure

12 shows injury curves and risk curves corresponding to different loading types for a fragile subject, and Figure 13 shows similar results for a stronger subject.

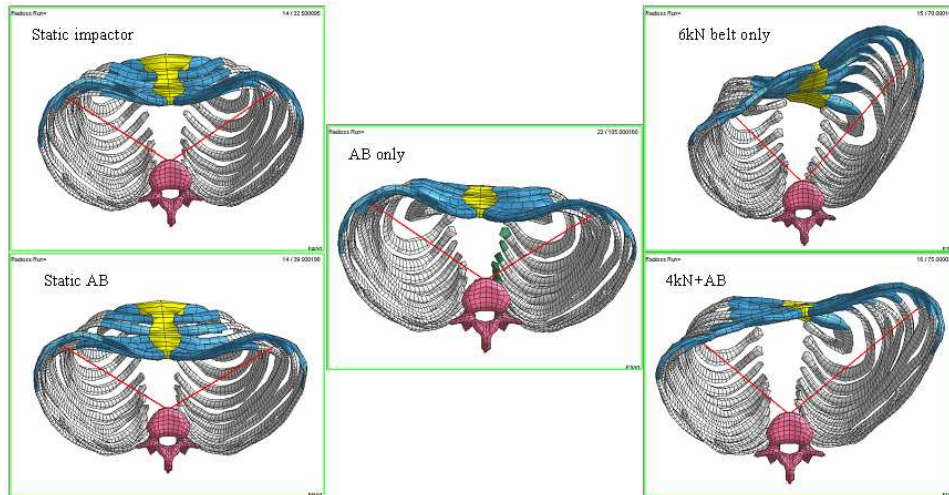


Figure 11. Ribcage deformation shape under different loading types based on the HUMOS2LAB simulations.

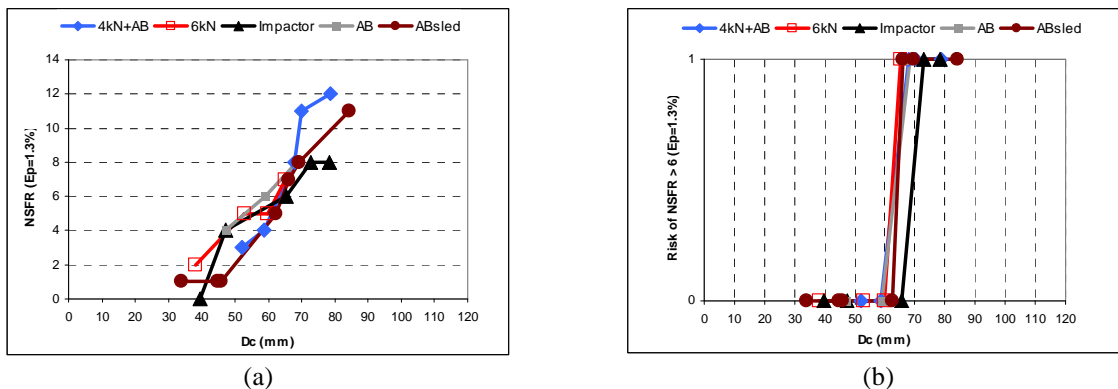


Figure 12. Injury curves (a) and risk curves of NSFR > 6 (b) with Dc as injury criterion. The plastic strain failure threshold was fixed at 1.3%, representing a fragile subject.

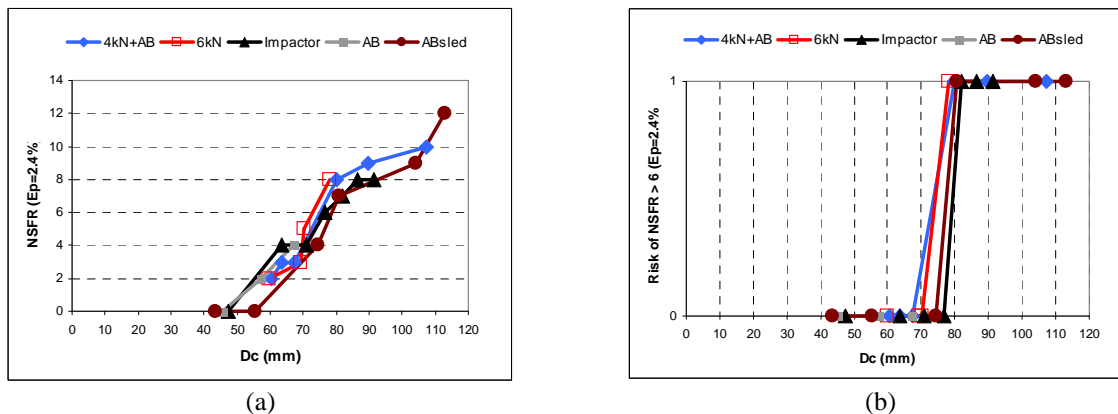


Figure 13. Injury curves (a) and risk curves of NSFR > 6 (b) with Dc as injury criterion. The plastic strain failure threshold was fixed at 2.4%, representing a stronger subject.

It can be observed that:

- The injury curve does not change significantly from one loading type to another.
- Risk curves of NSFR > 6 are reasonably close, especially when only sled tests are considered.
- The closeness between injury curves, but also between risk curves is much better with combined deflection than with sternal deflection.
- These observations are true both for a fragile subject (strain threshold at 1.3%) and also for a stronger subject (strain threshold at 2.4%).

A STRAIN-BASED INJURY CRITERION

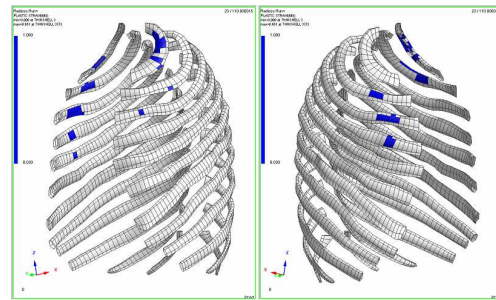
In the section related to injury mechanism, it was concluded that rib fractures can be explained by excessive strain level and that bending is the main component leading to high strain levels. This mechanism of rib fractures suggests that a strain (curvature)-based injury criterion could be used to evaluate rib fracture risk.

A first idea may be to use the maximum peak strain within the ribcage to predict rib fracture risk and severity. However, based on our simulations, we found that the maximum peak strain of ribs does not correlate with the number of fractured ribs. An example is provided below to illustrate this phenomenon.

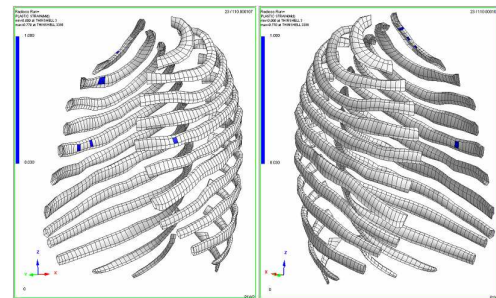
First, let's compare two simulations of sled tests, performed under identical crash conditions (a 50km/h, 0° frontal sled test): Simulation A corresponding to a 6kN shoulder load limiting belt only restraint, and Simulation B corresponding to a combined restraint with a 4 kN shoulder load limiting belt plus a driver airbag. Figure 14 shows predicted rib fractures for Simulation A and Simulation B. Elements in blue colour are those whose plastic strain went beyond the failure threshold fixed at 3%. The maximum peak strain is higher in Simulation A than in Simulation B. We can observe that there are five fractured ribs in Simulation A and one fractured rib in Simulation B. So, for the subject with a 3% plastic strain as the failure threshold, higher peak strain means also more fractured ribs.

Now let's examine the same simulations but with a more fragile subject (the failure strain fixed at 1.8%). The maximum peak strain is higher in Simulation A than in Simulation B. We can observe that there are eight fractured ribs in Simulation A and twelve fractured ribs in Simulation B (Figure 15). So, for the subject with a 1.8% plastic strain as

failure threshold, higher peak strain does not mean more fractured ribs.

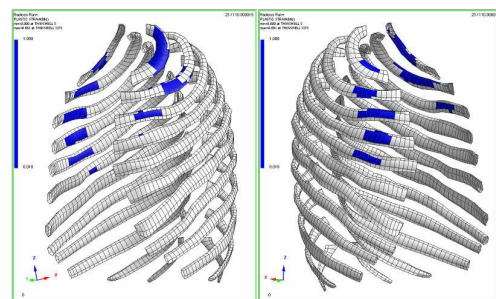


(a) Simulation A: LL6kN belt only

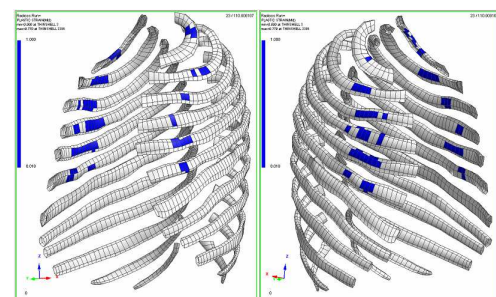


(b) Simulation B: LL4kN+AB

Figure 14. Rib fractures (blue elements) with plastic failure strain at 3%: (a) corresponding to a 6kN shoulder load limiting belt only restraint, and (b) corresponding to a 4kN shoulder load limiting belt plus airbag restraint.



(a) Simulation A: LL6kN belt only



(b) Simulation B: LL4kN+AB

Figure 15. Rib fractures (blue elements) with plastic failure strain at 1.8%: (a) corresponding to a 6kN shoulder load limiting belt only restraint, and (b) corresponding to a 4kN shoulder load limiting belt plus airbag restraint.

Based on the elements above, we propose to use the number of fractured ribs (NFR) as a global injury criterion. On the one hand, this number intrinsically reflects the injury level for the ribs, and on the other hand, it can be determined by strain measurement of each rib. However, a mechanical dummy does not mimic rib fractures. Besides, a mechanical dummy, such as the THOR or H-III, do not have the same number of ribs as the human. So, one may wonder how it is possible to apply such a criterion on a dummy.

Figure 16 illustrates a possible approach to use this criterion. The key point is to determine, for a given dummy, a strain threshold. For each rib of the dummy, once its maximal peak strain reaches the threshold, the rib will be considered as fractured. In this way, we can determine the number of fractured ribs for the dummy in question for each test. But what is the best way to determine the strain threshold? To do this, a three-step approach can be used. First, PMHS-dummy matched tests should be gathered, where we know rib fracture outcome of all PMHS tests, and where the strain distribution of each rib is measured. Then, the NFR-PMHS should be plotted versus the NFR-dummy determined by supposing a strain failure threshold. Finally, we should vary this strain failure threshold until the best correlation is identified. This strain threshold will be the threshold for this specific dummy. For another dummy, we can apply the same method to identify its proper strain threshold.

Once the strain threshold has been determined, the NFR can be derived easily and be used as an injury criterion in the same way as a traditional one, such as the sternal deflection: either to discriminate two restraints as showed in Figure 17-a, or to evaluate the injury risk by constructing risk curves (Figure 17-b). For example, a NFR of 1 may indicate that the risk of AIS \geq 3 is 20%. A NFR of 4 may indicate that the risk of AIS \geq 3 is 50%. However, it is important to keep in mind that

NFR(dummy) is equivalent to the number of ribs exceeding the strain threshold, which will be lower for the dummy than for PMHS because the dummy ribs will not fail and cause other ribs to be subjected to greater strain. Furthermore, it should be remembered that the THOR dummy has 14 ribs while human has 24. So, NFR(dummy) should be considered as a global indicator reflecting the severity of ribcage deformation.

Determining $\epsilon_{\text{threshold}}$ to obtain the best regression

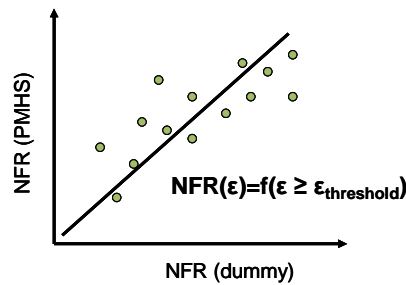
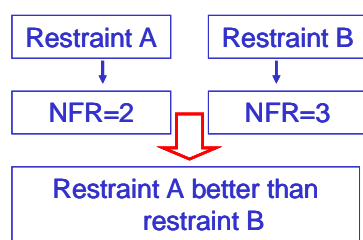


Figure 16. Scheme of a possible approach to apply the NFR as an injury criterion to dummies.

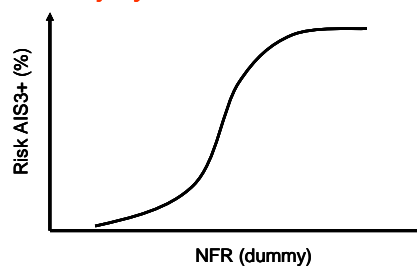
In order for the NFR to work on a mechanical dummy, a reasonable correlation between the NFR-PMHS and the NFR-Dummy should exist. This requirement implies that the dummy should be sensitive to ribcage strain distribution in a similar way to human bodies, and this similitude should be true for different types of loading and its tendency should follow the same trend as in human bodies versus impact severity. To prove this, a large amount of PMHS tests may need to be duplicated with the dummy equipped with strain gauges. But for a feasibility study, a demonstrator with a dummy model may be considered. For this purpose the simulation matrix, presented above for the HUMOS2LAB model, needs to be duplicated with the dummy model.

Discriminating 2 restraints



(a)

Injury risk assessment



(b)

Figure 17. Scheme illustrating how the NFR can be used to discriminate different restraints and to assess injury risk.

DISCUSSION

Effects of rib fracture modeling mode

In the HUMOS2LAB model, rib fractures are simulated by deleting shell elements representing cortical bone of ribs, once their plastic failure thresholds are reached. With a mechanical dummy, it is unrealistic to imagine, for the time being, a frangible ribcage. So, it is natural to ask if the Dc would work on a mechanical dummy. To investigate this question, simulations were run without deleting shell elements that reached the failure threshold. It is easy to understand that such an approach is more dummy-like but neglects in some extent the domino effects of rib fractures.

Injury curves and risk curves in terms of Dc are given in Figure 18 for a fragile subject and in Figure 19 for a stronger subject. It can be observed that restraint-dependency is considerable for the fragile subject, but is not significant for the stronger subject, especially when only restraints in a dynamic sled environment are taken into account. Although a more significant restraint-dependency was observed based on simulations without shell element deletion, the Dc remains globally better than the sternal deflection, and presents only a moderate restraint-dependency when considering the overview of injury curves corresponding to sled-related loading types.

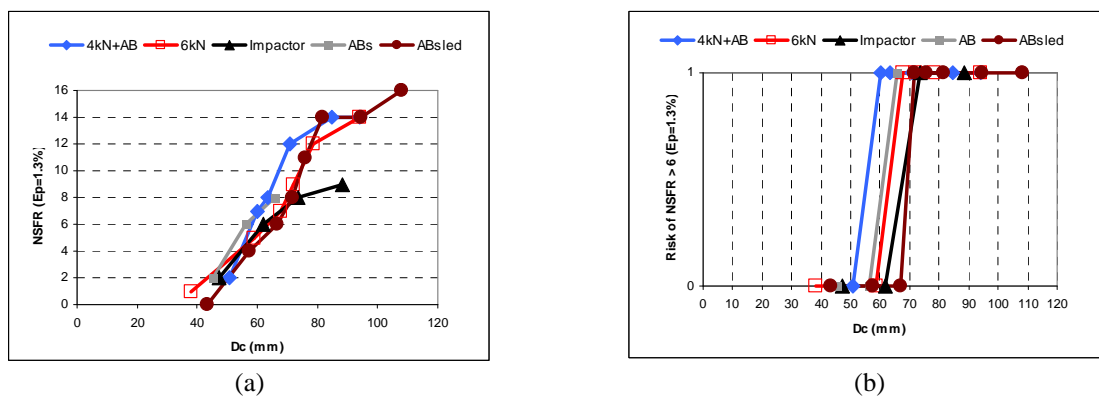


Figure 18. Injury curves (a) and risk curves of NSFR>6 (b) with Dc as injury criterion, based on simulations without element deletion. The plastic strain failure threshold was fixed at 1.3%, representing a fragile subject.

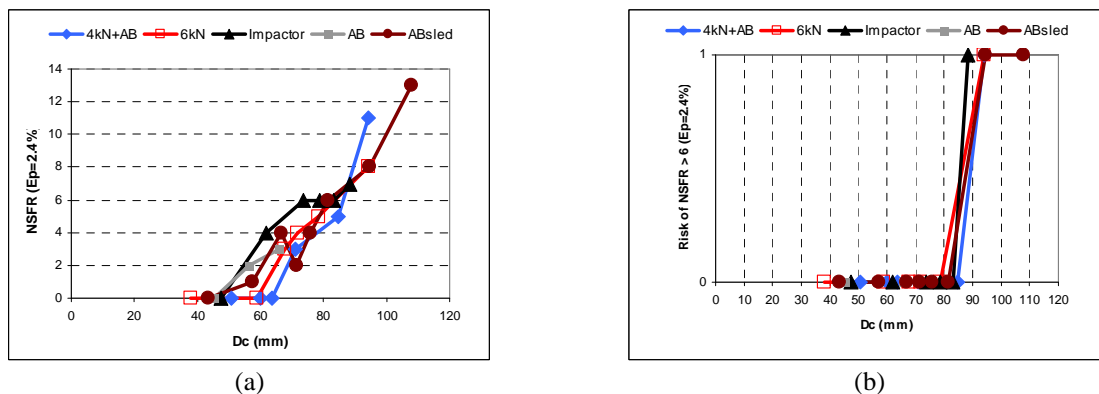


Figure 19. Injury curves (a) and risk curves of NSFR>6 (b) with Dc as injury criterion, based on simulations without element deletion. The plastic strain failure threshold was fixed at 2.4%, representing a stronger subject

Applicability of Dc to dummies

One important question is whether the Dc can be applied to mechanical dummies.

In Figure 20, THOR geometry and HUMOS2LAB geometry are compared. It can be noted that the two lower thoracic deflection measurements correspond,

in some extent, to the deflection measured at Ribs 7 of HUMOS2LAB model. The two upper deflection measurements can be used to approximate the mid-sternum deflection.

Petitjean et al. (2002) performed THOR and H-III sled tests. For the THOR dummy, they found a 47 mm differential deflection for the 6 kN belt only

restraint and a 37 mm differential deflection for the 4kN+AB restraint. Even for the H-III dummy, they found also the existence of differential deflection: 15 mm with the 6kN restraint and 8 mm with the 4kN+AB restraint.

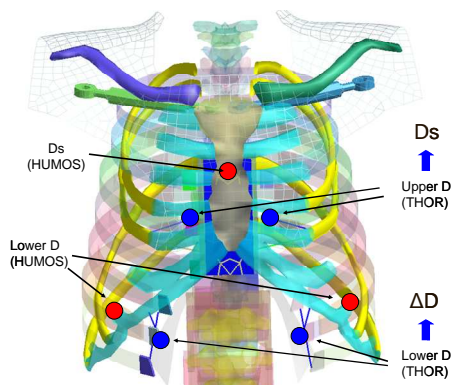


Figure 20. Comparison of the THOR dummy (NHTSA THOR FE model) geometry to the HUMOS2LAB model.

So, in principle, the combined deflection can be calculated with current THOR dummy. However, it is unknown if the criterion measured with the dummy remains valid, i.e. keeps its insensitivity to loading types, as it is the case with HUMOS2LAB model.

To verify this, the most direct method is to gather matched PMHS-THOR test data and to construct risk curves for different types of loading.

Again, an alternative is to use a model of THOR dummy to duplicate simulations performed with HUMOS2LAB.

Choices of Lc and Cf

Lc and Cf are two parameters which determine how the differential deflection of the lower thorax should contribute to the combined deflection. In the results and discussions above, Lc was fixed at 24 mm and Cf at 0.15 for both fragile and resistant subjects. However, there is no reason that these parameters should be the same between fragile and resistant subjects. By using population-oriented Lc and Cf, the restraint-independency of the Dc can be further improved. Regarding the application of Dc on a mechanical dummy, it is obvious that specific Lc and Cf should be determined.

Applicability of NFR to dummies

In order to give a first indication as to whether the criterion NFR may be applied to a dummy, a preliminary study was carried out on THOR dummy. The THOR dummy was instrumented with strain gauges: 20 gauges for each rib ring. It was

loaded from the front with the conventional 23.4 kg cylinder impactor at 4.3 m/s. Strain measurements were then used to calculate the strain profile for each rib ring. These strains profiles were compared to strain profiles derived from PMHS tests in the same loading conditions. Figure 21 shows an example of the comparisons: the blue curve represents strain distribution in THOR test, and the two other curves represent the strain distribution in two PMHS tests. The strain measured on the THOR being much lower than the strain measured in PMHS tests, the original THOR strain was tripled in the blue curve in Figure 21 to enable the comparison. First positive signs for implementing the NFR on THOR dummy can be observed in the figure: the strain distribution on the THOR rib was correctly measured by using strain gauges; and the distribution has the potential to be transformed to reflect PMHS rib strain profile.

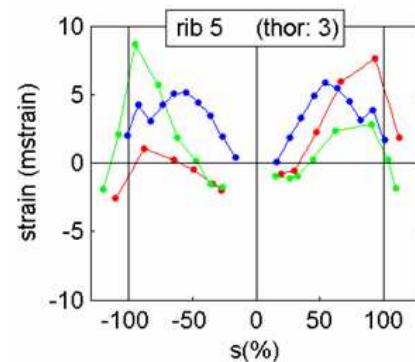


Figure 21. Strain distribution along the 3rd THOR ribs (blue) compared to corresponding 5th ribs on PMHS. Original THOR strain measurement was tripled to enable the comparison.

Limitations of the study

Findings and recommendations in the study were based on human body model simulations. They are results of a series of exploration activities, which were made possible by exploiting advantages of human body model approach. Results are more indicative than confirmative. They should be checked in particular with respect to experimental data when they become available.

CONCLUSIONS

An existing human model was updated and validated for frontal impact simulation, not only in terms of its gross motion response, but also in terms of its capability to predict rib fractures. A series of simulations using the model were performed, forming a “virtual” PMHS test database. Five loading types were covered by this database: three point shoulder-lap belt restraint, combined three point shoulder-lap belt and airbag restraint, and airbag only restraint in a dynamic sled test

environment, and airbag and cylindrical impactor loading in a static environment. For each simulation, the rib fracture outcome was established and different metrics of ribcage deflection were recorded.

Based on these “virtual” PMHS tests, excessive strain, mainly generated by bending, was identified as a primary mechanism of rib fractures.

It was found that maximum peak strain of ribs does not predict the number of fractured ribs correctly. It was suggested to use the NFR (Number of Fractured Ribs) directly as a global injury criterion. A scheme to use the NFR on a mechanical dummy, where ribs always remain in the elastic state, is proposed. The NFR offers the potential to be a universal injury criterion – restraint-independent, impact direction-independent and suitable for evaluating different levels of injuries.

A more usual metric, named as Combined Deflection and noted as D_c , is also proposed. This metric is a global deflection-based predictor for serious injury (more than six fractured ribs). Injury curves and risk curves constructed with this criterion do not vary significantly from one loading type to another. It has potential as a candidate for a restraint-independent injury predictor.

ACKNOWLEDGEMENTS

This work was performed in the framework of the EU funded FP7 THORAX project. The authors would like to thank the EU-Commission for the funding and the project partners for their collaboration.

REFERENCES

Bose, D., Pipkorn, B., Crandall, J., Lessley, D., Trowbridge, M. (2009) Multi-point thoracic deflection measurement as a predictor of rib injury in frontal collision. Proc. 30th International Workshop on Human Subjects for Biomechanical Research, Savannah, GA.

Bouquet, R., Ramet, M., Bermond, F., Caire, Y., Talantikite, Y., Robin, S. and Voiglio, E. (1998) Pelvis human responses to lateral impact. Proc. ESV1998.

Burstein, A.H. et al. (1976) Aging of bone tissue : mechanical properties. *Journal of Bone and Joint Surgery* 58(A): 82.

Kent, R., Lessley, D., Shaw, G., and Crandall, J. (2003) The utility of H-III and THOR chest deflection for discriminating between standard and force-limiting belt systems. *Stapp Car Crash Journal* 47: 267-297.

Kent R., Patrie J., Poteau F., Matsuoka F., Mullen C., ‘Development Of An Age-Dependent Thoracic Injury Criterion For Frontal Impact Restraint Loading’ Paper No. 72, ESV Conference, Nagoya, Japan 2003.

Kimpara, H., Lee, J.B., Yang, K.H., King, A.I., Iwamoto, M., Watanabe, I., and Miki, K. (2005) Development of a three-dimensional finite element chest model for the 5th percentile female. *Stapp Car Crash Journal* 49: 251-269.

Kroell, C., Schneider, D., Nahum, A. (1974) Impact Tolerance Of The Human Thorax II. . Proc. 18th Stapp Car Crash Conference, pp. 84-134. Society of Automotive Engineers, Warrendale, PA.

Lizee, E., Robin, S., Song, E., Bertholon, N., Le Coz, J.Y., Besnault, B. and Lavaste, F. (1998) Development of a 3D finite element model of the human body. Proc. 42nd Stapp Car Crash Conference, pp.115-138. Society of Automotive Engineers, Warrendale, PA.

Petitjean, A., Lebarbé, M., Potier, P., Trosseille, X., Lassau, J-P. (2002) Laboratory reconstructions of real world frontal crash configurations using the H-III and THOR dummies and PMHS. *Stapp Car Crash Journal* 46: 27-54.

Robin (2001). HUMOS: Human model for safety - A joint effort towards the development of refined human-like car occupant models. Proc. of the 17th Int. Tech. Conf. on the Enhanced Safety of Vehicles, Paper Number 297.

Shaw, G. et al. (2009) Rib Impact response of Restrained PMHS in frontal sled tests: Skeletal deformation patterns under seat belt loading. *Stapp Car Crash Journal* 53: 1-48.

Song, E., Trosseille, X., Baudrit, P. (2009) Evaluation of thoracic deflection as an injury criterion for side impact using a finite elements thorax model. *Stapp Car Crash Journal* 53: 155-191.

Trosseille, X., Baudrit, P., Lepout, T., Petitjean, A., Potier, P., Vallancien, G. (2009) The effect of angle on the chest injury outcome in side loading. *Stapp Car Crash Journal* 53: 403-419.

Veziin, P., Verriest, J.P. (2005) Development of a set of numerical human model for safety. Proc. of the 19th Int. Tech. Conf. on the Enhanced Safety of Vehicles, Paper Number (05-0163).

APPENDIX A

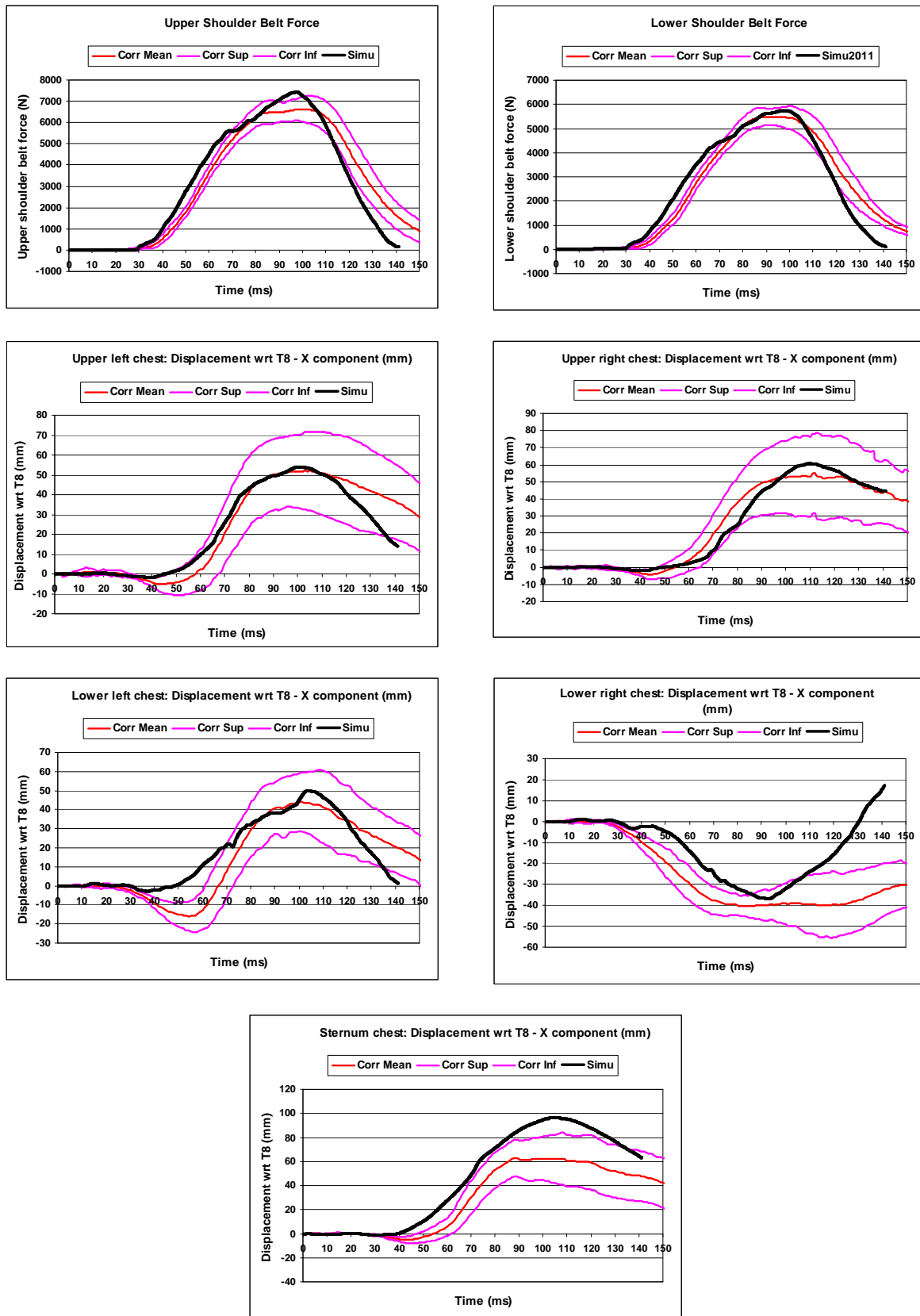


Figure A1. Comparison of HUMOS2LAB model responses to corridors based on sled tests with belt only restrained cadavers performed by Shaw et al. 2009. The corridors were derived by Lebarbé et al. in the framework of ISO WG5.

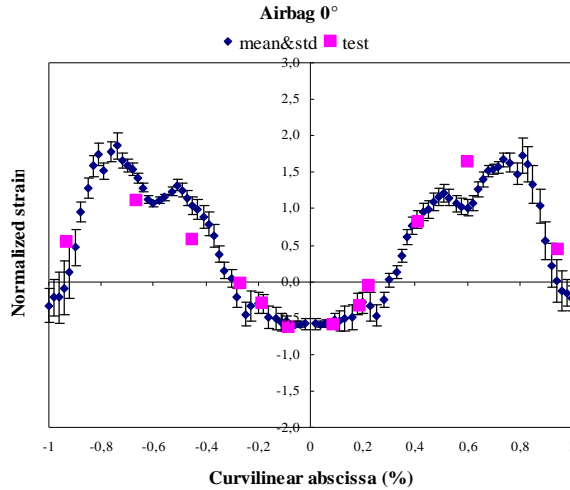


Figure A2. Comparison of the strain profile for the 5th rib between the HUMOS2LAB model and the cadaver tests under static airbag loading performed by Trosseille et al. 2009.

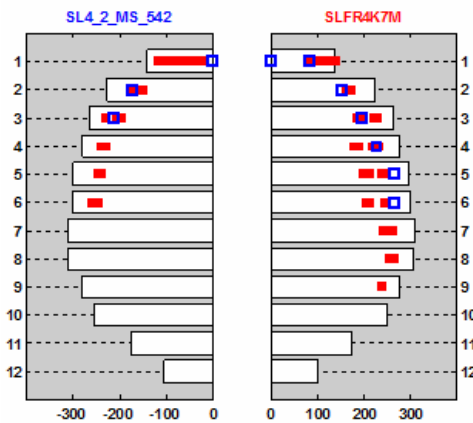


FIGURE A3. Comparison of the fracture regions between the HUMOS2LAB model (red) and the cadaver sled test MS_542 (blue) under combined 4kN belt load limiter and airbag restraint performed by Petitjean et al. 2002.

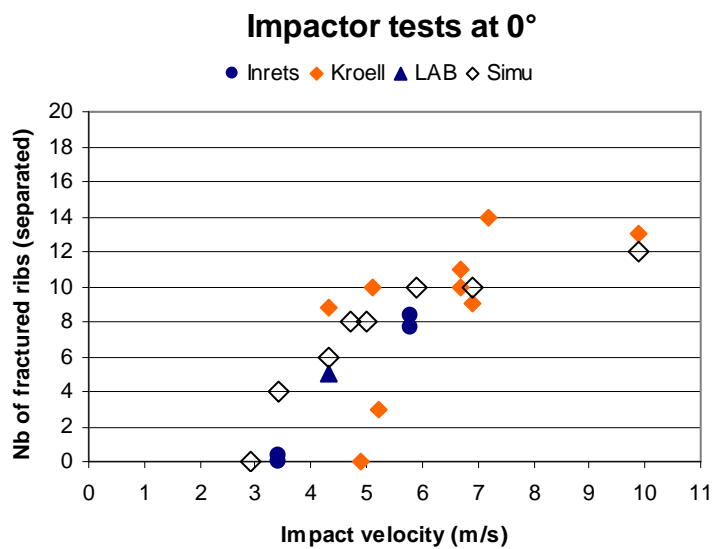


FIGURE A4. Number of fractured ribs versus loading severity for impactor tests: comparison between the HUMOS2LAB model and the experimental data (Kroell et al. 1974, Bouquet et al. 1998, Trosseille et al. 2009).

Table A1.

Simulation matrix performed with plastic strain threshold of 1.3%

Plastic strain = 1.3%				
Model name	Test config	Severity	Loading type	NFR
20AB4R8R	Sled test	$\Delta V=20\text{km/h}$	4kN belt+AB	3
22AB4R8R	Sled test	$\Delta V=22\text{km/h}$	4kN belt+AB	4
23AB4R8R	Sled test	$\Delta V=23\text{km/h}$	4kN belt+AB	8
25AB4R8R	Sled test	$\Delta V=25\text{km/h}$	4kN belt+AB	11
30AB4R8R	Sled test	$\Delta V=30\text{km/h}$	4kN belt+AB	12
20FD6R8R	Sled test	$\Delta V=20\text{km/h}$	6kN belt only	2
25FD6R8R	Sled test	$\Delta V=25\text{km/h}$	6kN belt only	5
28FD6R8R	Sled test	$\Delta V=28\text{km/h}$	6kN belt only	5
30FD6R8R	Sled test	$\Delta V=30\text{km/h}$	6kN belt only	7
30AB0R8R	Sled test	$\Delta V=30\text{km/h}$	AB only, Δp^* , m(t)**	1
40AB0R8R	Sled test	$\Delta V=40\text{km/h}$	AB only, Δp , m(t)	1
40AB488R	Sled test	$\Delta V=40\text{km/h}$	AB only, $1.07\Delta p$, m(t)	1
40AB508R	Sled test	$\Delta V=40\text{km/h}$	AB only, $1.11\Delta p$, m(t)	5
40AB528R	Sled test	$\Delta V=40\text{km/h}$	AB only, $1.15\Delta p$, m(t)	7
40AB3R8R	Sled test	$\Delta V=40\text{km/h}$	AB only, $1.22 \Delta p$, m(t)	8
40AB1R8R	Sled test	$\Delta V=40\text{km/h}$	AB only, $1.44\Delta p$, m(t)	11
F29STR8R	Impactor	Vimpact=2.9m/s	15cm&23.4kg disc	0
F34STR8R	Impactor	Vimpact=3.4m/s	15cm&23.4kg disc	4
F43STR8R	Impactor	Vimpact=4.3m/s	15cm&23.4kg disc	6
F47STR8R	Impactor	Vimpact=4.7m/s	15cm&23.4kg disc	8
F50STR8R	Impactor	Vimpact=5.0m/s	15cm&23.4kg disc	8
OPM12R8R	Static airbag	AB/PMHS=128mm	Unfolded AB	8
OPM15R8R	Static airbag	AB/PMHS=158mm	Unfolded AB	6
OPM17R8R	Static airbag	AB/PMHS=178mm	Unfolded AB	4

* Δp =differential pressure for venting; ** m(t)=mass flow law

Table A2.

Simulation matrix performed with plastic strain threshold of 2.4%

Plastic strain = 2.4%				
Model name	Test config	Severity	Loading type	NFR
30AB4R8Q	Sled test	$\Delta V=30\text{km/h}$	4kN belt+AB	2
40AB4R8Q	Sled test	$\Delta V=40\text{km/h}$	4kN belt+AB	3
45AB4R8Q	Sled test	$\Delta V=45\text{km/h}$	4kN belt+AB	3
47AB4R8Q	Sled test	$\Delta V=47\text{km/h}$	4kN belt+AB	8
50AB4R8Q	Sled test	$\Delta V=50\text{km/h}$	4kN belt+AB	9
60AB4R8Q	Sled test	$\Delta V=60\text{km/h}$	4kN belt+AB	10
30FD6R8Q	Sled test	$\Delta V=30\text{km/h}$	6kN belt only	2
40FD6R8Q	Sled test	$\Delta V=40\text{km/h}$	6kN belt only	3
45FD6R8Q	Sled test	$\Delta V=45\text{km/h}$	6kN belt only	5
50FD6R8Q	Sled test	$\Delta V=50\text{km/h}$	6kN belt only	8
40AB0R8Q	Sled test	$\Delta V=40\text{km/h}$	AB only, Δp^* , m(t)**	0
40AB3R8Q	Sled test	$\Delta V=40\text{km/h}$	AB only, $1.44\Delta p$, m(t)	0
43AB3R8Q	Sled test	$\Delta V=43\text{km/h}$	AB only, $1.44\Delta p$, m(t)	4
45AB3R8Q	Sled test	$\Delta V=45\text{km/h}$	AB only, $1.44\Delta p$, m(t)	7
50AB1R8Q	Sled test	$\Delta V=50\text{km/h}$	AB only, $1.44\Delta p$, $1.3m(t)$	9
50AB2R8Q	Sled test	$\Delta V=50\text{km/h}$	AB only, $1.89\Delta p$, $1.6m(t)$	12
F34STR8Q	Impactor	Vimpact=3.4m/s	15cm&23.4kg disc	0
F43STR8Q	Impactor	Vimpact=4.3m/s	15cm&23.4kg disc	4
F47STR8Q	Impactor	Vimpact=4.7m/s	15cm&23.4kg disc	4
F50STR8Q	Impactor	Vimpact=5.0m/s	15cm&23.4kg disc	6
F53STR8Q	Impactor	Vimpact=5.3m/s	15cm&23.4kg disc	7
F56STR8Q	Impactor	Vimpact=5.6m/s	15cm&23.4kg disc	8
F59STR8Q	Impactor	Vimpact=5.9m/s	15cm&23.4kg disc	8
OPM12R8Q	Static airbag	AB/PMHS=128mm	Unfolded AB	4
OPM15R8Q	Static airbag	AB/PMHS=158mm	Unfolded AB	2
OPM17R8Q	Static airbag	AB/PMHS=178mm	Unfolded AB	0

* Δp =differential pressure for venting; ** m(t)=mass flow law